Self-limited growth of laser-induced vapor bubbles around single microabsorbers

Jörg Neumann[a] and Ralf Brinkmann
Medizinisches Laserzentrum Lübeck GmbH, Peter-Monnik-Weg 4, D-23562 Lübeck, Germany

(Received 7 March 2008; accepted 17 June 2008; published online 22 July 2008)

Laser-induced bubble dynamics around micrometer-sized absorbers in water is studied. A single transient microbubble forms around the whole laser-heated particle due to vaporization of the surrounding water. Using 12 ns laser pulses, the bubble size increases with radiant exposure, whereas for 240 and 1800 ns pulses multiple bubble oscillations with a maximum bubble diameter are observed, which is almost independent from the applied radiant exposure. In this case, thermal decoupling of the expanding bubble from the absorber by the insulating vapor limits the heat transfer from the particle to the bubble. The resulting self-limited bubble growth can increase the precision of cellular laser microsurgery. © *2008 American Institute of Physics*. [DOI: 10.1063/1.2957030]

In many technical procedures such as bubble-jet printer technologies,[1,2] steam laser cleaning,[3,4] bubble induced optical limiting, and switching in suspensions[5,6] a fluid vaporizes at a rapidly heated solid surface and bubbles form on the micro- or nanoscale. For biomedical applications, endogenous and exogenous micro- or nanoabsorbers are utilized to cause selective tissue damage on the cellular level.[7,8] In this regime of selective photothermolysis, the absorbers are heated in a transparent surrounding by pulsed laser irradiation, which causes high temperatures spatially confined to the absorbers. In liquid environments, the resulting transient vapor bubbles induce highly localized thermomechanical damage to biological structures.[9] This technique has been successfully applied in medical procedures such as selective retina therapy[10] (SRT) and selective laser trabeculoplasty[11] where cells containing absorbing pigments (melanosomes) are targeted selectively for destruction. Damage to the adjacent nontargeted cells, e.g., photoreceptor cells in SRT, has to be avoided. The positive therapeutic effect is induced by the healing response of the tissue. Using exogenous bioconjugated absorbers, this technique is proposed for selective cell killing in anticancer therapy[12–14] and generation of subcellular effects such as selective protein knockdown[15] or cell membrane permeabilization.[16] All aforementioned selective effects are mediated by bubble formation around laser-heated absorbers. The bubble size determines the damage range in the tissue. Therefore, we study the bubble dynamics around micrometer-sized absorbers with respect to laser pulse duration and radiant exposure to find optimum irradiation parameters, i.e., to keep the damage range constant for a broad range of radiant exposure ensuring a well-defined precision of selective photothermolysis.

As a model system for SRT, we suspend micrometer-sized melanosomes from retinal pigment epithelial cells of porcine eyes in water. The suspension is irradiated by pulsed lasers with full width at half maximum pulse durations τ_{laser} of 12 ns at a wavelength of 532 nm, of 240 and 1800 ns at 527 nm, which are far below and close to the particle's thermal relaxation time τ_T. These pulse durations ensure spatially confined heating, but exclude inertially confined irradiation, which avoids tissue damaging shock waves,[17] i.e., $\tau_{\text{ac}}=2R/c\approx 700\ \text{ps}\ll\tau_{\text{laser}}\lesssim\tau_T=R^2/4\kappa_{\text{H}_2\text{O}}\approx 440\ \text{ns}$ with particle radius $R\approx 0.5\ \mu\text{m}$, heat diffusivity of water $\kappa_{\text{H}_2\text{O}}$ and speed of sound c.[18] Thus, for the laser pulse parameters used in this study, bubble formation is the origin of cell death[19] and bubble dynamics determines the damage range in the tissue.

Spatially homogeneous irradiation with a flat top beam profile is achieved in the suspension by mapping the fiber tip for laser pulse delivery into the melanosome suspension. The size of the laser-induced bubble is determined by time-resolved microscopy using a 3 ns dye-laser pulse for illumination, which is triggered at an adjustable delay related to the green irradiation laser pulse (Fig. 1, for details see Ref. 18). The temporal bubble dynamics is observed by means of the transmission of a probe laser beam, which is focused onto a single melanosome. During the bubble lifetime, light is scattered out of the detection aperture of the receiver photodiode, which results in a decreased detected probe laser power. The fast flash photographs deliver the size of the bubble at a specific time, whereas the light scattering technique provides the lifetime of the bubble.

The bubble dynamics strongly depends on the irradiation laser pulse duration (Fig. 2). Due to heat diffusion out of the absorber during the laser pulse ($\tau_T\lesssim\tau_{\text{laser}}$ for 240 and 1800 ns), the threshold radiant exposure for bubble formation increases with pulse duration (Fig. 2, second row). Increasing radiant exposure leads to a larger heating rate and an earlier onset of bubble growth relative to the laser pulse at constant pulse duration (Fig. 2, each column), because the bubble nucleation temperature of about 150 °C (Ref. 18) is reached earlier. For 12 ns pulses, increasing radiant exposure leads to a single bubble with increasing lifetime [Fig. 2(a)].

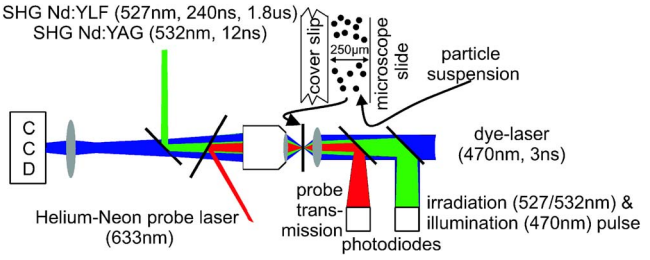

FIG. 1. (Color online) Experimental setup.

[a]Electronic mail: j.neumann@lzh.de.

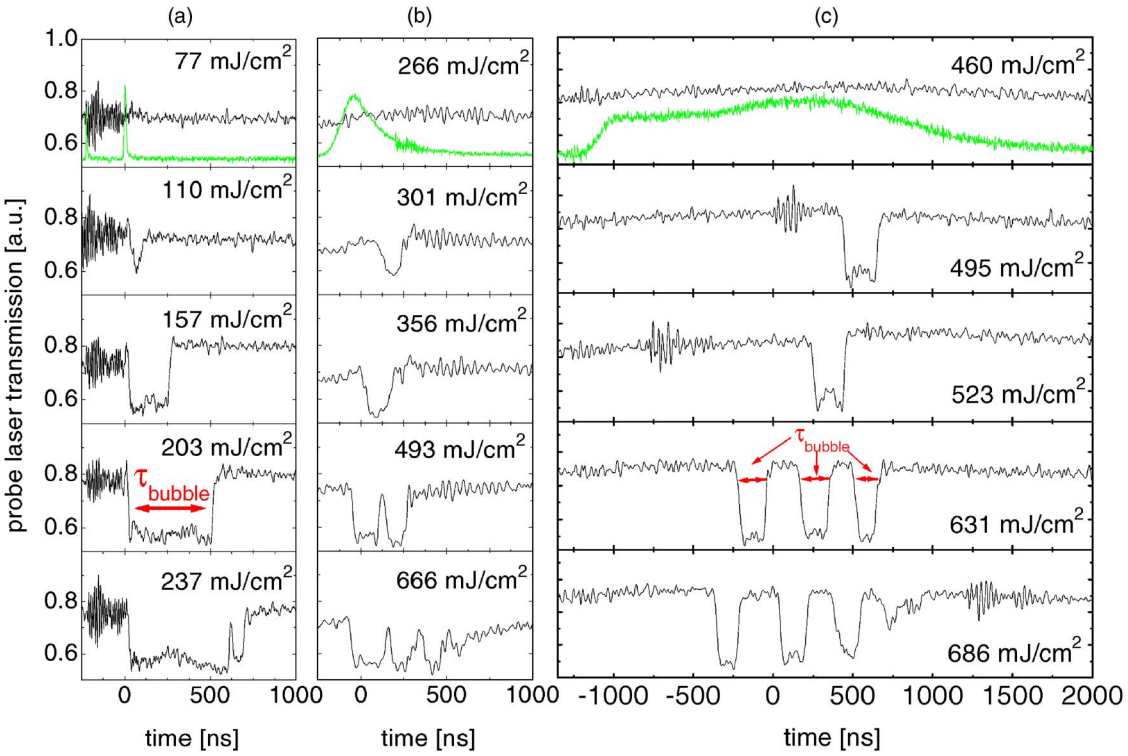

FIG. 2. (Color online) Probe laser transmission for melanosomes irradiated by 12 ns (a), 240 ns (b), and 1800 ns (c) laser pulses. The same melanosome was irradiated with increasing radiant exposure at the same pulse duration for each column. Each dip in the probe laser transmission corresponds to a bubble. In addition, the laser pulse shape for particle heating is plotted in the top row.

Occasionally, a bubble rebound with a significant smaller lifetime occurs after the collapse of the first bubble [Fig. 2(a), 237 mJ/cm^2]. Applying 240 and 1800 ns pulses, multiple bubble oscillations can be observed with increasing radiant exposure, but the lifetime of these bubbles τ_{bubble} is nearly independent from the radiant exposure [Figs. 2(b) and 2(c)]. Only the number of bubble oscillations increases with radiant exposure.

Utilizing an interferometric technique,[20] the bubble dynamics has been proven to be temporally symmetrically, i.e., the maximum bubble diameter $d_{\text{bubble}}^{\max}$ during each oscillation is observed at 50% of its lifetime. Fast flash photographs were taken at $(0.5 \pm 0.1)\tau_{\text{bubble}}$ (Fig. 3) to assess the maximum bubble diameter as an estimation for the damage range in the tissue. A linear relationship between bubble size and lifetime is obtained demonstrating that lifetime is a measure for the size (Fig. 3). All data fit the Rayleigh equation[21] for inertia limited bubble dynamics. In case of 240 and 1800 ns pulses, the maximum bubble diameter is limited to 3 μm, whereas diameters up to 7 μm were observed at $\sim$350 mJ/cm^2 for 12 ns pulses (Fig. 3). At higher radiant exposure thermal disintegration of the melanosome accompanied by permanent bubble formation due to the production of noncondensable gas occurred for 12 ns pulses.

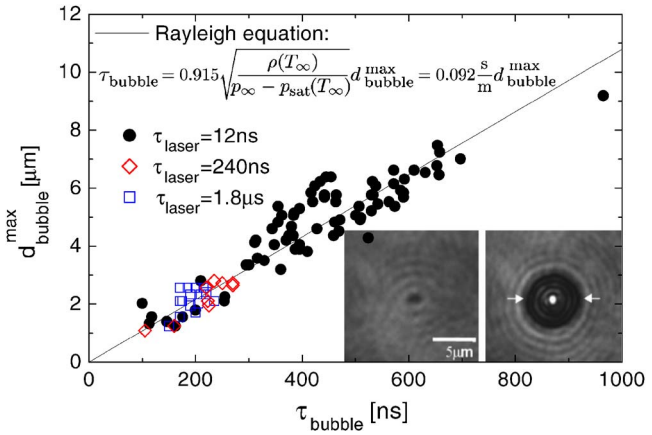

FIG. 3. (Color online) Plot of the Rayleigh equation (with ambient pressure p_∞=101 kPa, saturated vapor pressure $p_{\text{sat}}(20\,^\circ\text{C})$=2.33 kPa, water density $\rho(20\,^\circ\text{C})$=998 kg/m^3) and plot of the measured maximum bubble diameters around melanosomes at $(0.5 \pm 0.1)\tau_{\text{bubble}}$. Photographs of a melanosome before irradiation (left) with a 12 ns pulse at 369 mJ/cm^2 and the corresponding bubble (τ_{bubble}=533 ns) around the same melanosome (right) at 255 ns after nucleation are shown.

The observation of multiple bubble oscillations can be explained in a qualitative model. When the nucleation temperature is reached after a certain period of laser-induced heating, bubbles nucleate in the metastable water at the particle surface and coalesce to a vapor blanket around the whole particle.[22] The vapor thermally insulates the absorber,[23–25] because the heat diffusivity of vapor is significantly smaller than of liquid water.[26,27] During the expansion phase of inertia limited bubble dynamics, the vapor pressure drives the bubble growth. Only the surrounding metastable water, which was conductively heated by the particle before bubble nucleation, can vaporize at the bubble interface and increase the kinetic energy of the bubble. Now, the bubble dynamics is nearly decoupled from the particle due to the insulating vapor. The vaporization at the bubble interface consumes latent heat and cools the thermal boundary layer around the bubble. Additionally, this thermal boundary layer thins during bubble expansion due to growth of its surface area and heat diffusion in the surrounding.[23] When the thermal boundary layer cools down, the vapor inside the bubble condenses at the vapor-water interface. The vapor pressure inside the bubble and therefore its expansion velocity decreases, which finally results in bubble contraction. When the

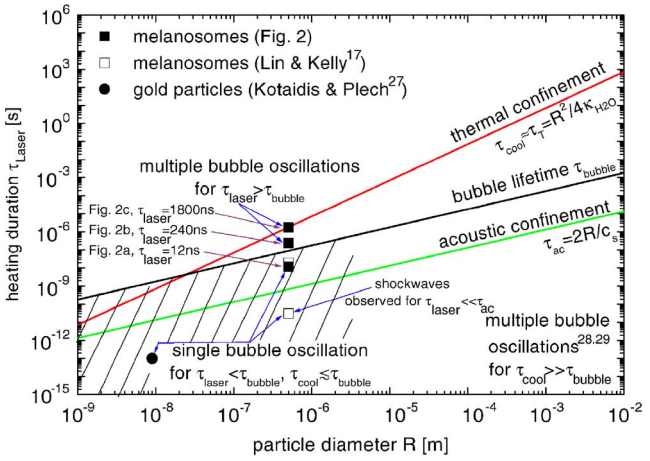

FIG. 4. (Color online) Multiple bubble oscillations can occur either for small particles, when the heating duration (τ_{laser}) is longer than the bubble lifetime (approximated by the Rayleigh equation), or for larger particles, when the characteristic cooling time (τ_{cool}) is larger than the bubble lifetime. The area in which single bubble oscillations are expected is dashed.

bubble has collapsed completely, water gets into contact with the hot particle again. For 240 and 1800 ns pulses, the laser still heats the particle after the bubble collapse. The nucleation temperature, which is nearly independent from the heating rate,[18] i.e., applied radiant exposure, can be reached again after the collapse and an additional bubble oscillation is initiated. Thus, the main parameter influencing the bubble dynamics for a given absorber size is not the applied radiant exposure, but the thermal boundary layer around the particle at nucleation. The nucleation temperature determines the initial vapor pressure in the bubble and the thickness of the thermal boundary layer indicates the amount of stored energy for bubble growth. Slightly above bubble threshold radiant exposure, the lifetime and size of the bubble increase with pulse duration (Fig. 2, second row), because the thermal boundary layer thickness increases with heating duration required for bubble nucleation. For 12 ns pulses, the bubble size depends on radiant exposure, which indicates that the energy transfer to the bubble is faster than the time for thermal decoupling of the melanosome from the bubble due to insulating vapor. In this case, the applied radiant exposure determines the bubble size.

The conditions for multiple bubble oscillations around microabsorbers can be analyzed in a more general way (Fig. 4). For 12 ns irradiation, the storable energy in the microabsorber, which is limited by its cooling time τ_{cool} and the maximum absorber temperature without occurrence of thermal absorber disintegration, is not sufficient to cause major multiple oscillations after the laser pulse [$\tau_{laser} < \tau_{bubble}$ and $\tau_{cool} \lesssim \tau_{bubble}$ in Fig. 4, compare Fig. 2(a)]. Immersion of hot macroscopic metal spheres with diameters of a few centimeters, which have a larger volume to surface ratio, into water without further heating of the sphere results in multiple oscillating bubbles (pulsational boiling) on the surface[28] ($\tau_{cool} \gg \tau_{bubble}$ in Fig. 4). This reveals that in the macroscopic case a sufficient amount of heat can be stored in the particle to produce multiple oscillations,[29] because the heat capacity of the absorber depends on its volume ($\propto R^3$) and the heat loss of the particle depends on its surface area ($\propto R^2$). For microabsorbers pulsational boiling can only be achieved, if the heating pulse is longer than the bubble lifetime [$\tau_{laser} > \tau_{bubble}$ in Fig. 4, compare Figs. 2(b) and 2(c)].

In biomedical applications, where highly selective targeting of cells is required without any collateral damage to neighboring structures, it has to be taken into account that microabsorbers often show variations in size and absorption. Moreover, scattering objects or other pigments in the tissue shadow the targeted absorbers. Thus, the required radiant exposure for bubble formation is unpredictable and has a large variation. For few nanosecond pulse duration, the bubble size is a function of the radiant exposure at the particle resulting in uncontrollable bubble sizes, which can lead to collateral damage of nontargeted cells. The application of pulses with a duration of a few hundred nanoseconds ($\tau_{bubble} \lesssim \tau_{laser} \lesssim R^2/4\kappa_{H_2O}$), e.g. for SRT,[10] can confine the thermal as well as the bubble induced damage range and provide a larger safety range for the applied radiant exposure, because the bubble size does not depend on radiant exposure.

[1] R. Allen, J. Meyer, and W. Knight, Hewlett-Packard J. **36**, 21 (1985).
[2] K. Balss, C. Avedisian, R. Cavicchi, and M. Tarlov, Langmuir **21**, 10459 (2005).
[3] K. Imen, S. Lee, and S. Allen, Appl. Phys. Lett. **58**, 203 (1991).
[4] F. Lang, P. Leiderer, and S. Georgiou, Appl. Phys. Lett. **85**, 2759 (2004).
[5] R. Hollins, Curr. Opin. Solid State Mater. Sci. **4**, 189 (1999).
[6] G. Eyring and M. Fayer, J. Appl. Phys. **55**, 4072 (1984).
[7] C. Lin, M. Kelly, S. Sibayan, M. Latina, and R. Anderson, IEEE J. Sel. Top. Quantum Electron. **5**, 963 (1999).
[8] C. Pitsillides, E. Joe, X. Wei, R. Anderson, and C. Lin, Biophys. J. **84**, 4023 (2003).
[9] R. Anderson and J. Parrish, Science **220**, 524 (1983).
[10] R. Brinkmann, J. Roider, and R. Birngruber, Bull. Soc. Belge Ophtalmol. **302**, 51 (2006).
[11] M. Latina and J. Tumbocon, Curr. Opin. Ophthal. **13**, 94 (2002).
[12] D. Leszczynski, C. Pitsillides, R. Pastila, R. Anderson, and C. Lin, Radiat. Res. **156**, 399 (2001).
[13] V. Zharov, R. Letfullin, and E. Galitovskaya, J. Phys. D: Appl. Phys. **38**, 2571 (2005).
[14] D. Lapotko, E. Lukianova, and A. Oraevsky, Lasers Surg. Med. **38**, 631 (2006).
[15] G. Hüttmann, J. Serbin, B. Radt, B. Lange, and R. Birngruber, Proc. SPIE **4257**, 398 (2001).
[16] C. Yao, R. Rahmanzadeh, E. Endl, Z. Zhang, G. Gerdes, and G. Hüttmann, J. Biomed. Opt. **10**, 019506 (2005).
[17] C. Lin and M. Kelly, Appl. Phys. Lett. **72**, 1 (1998).
[18] J. Neumann and R. Brinkmann, J. Biomed. Opt. **10**, 024001 (2005).
[19] H. Lee, C. Alt, C. Pitsillides, and C. Lin, J. Biomed. Opt. **12**, 064034 (2007).
[20] J. Neumann and R. Brinkmann, J. Biomed. Opt. **11**, 041112 (2006).
[21] M. Plesset and A. Prosperetti, Annu. Rev. Fluid Mech. **9**, 145 (1977).
[22] J. Neumann and R. Brinkmann, J. Appl. Phys. **101**, 114701 (2007).
[23] V. Pustovalov and B. Jean, Laser Phys. **16**, 1011 (2006).
[24] V. Kotaidis, C. Dahmen, G. von Plessen, F. Springer, and A. Plech, J. Chem. Phys. **124**, 184702 (2006).
[25] M. Hu, H. Petrova, and G. Hartland, Chem. Phys. Lett. **391**, 220 (2004).
[26] See http://www.iapws.org for technical standard "Revised Release on the IAPS Formulation 1985 for the Thermal Conductivity of Ordinary Water Substance" (IAPWS, London, UK, 1998).
[27] V. Kotaidis and A. Plech, Appl. Phys. Lett. **87**, 213102 (2005).
[28] J. Stevens and L. Witte, Int. J. Heat Mass Transfer **16**, 669 (1973).
[29] S. Board, A. Clare, R. Duffey, R. Hall, and D. Poole, Int. J. Heat Mass Transfer **14**, 1631 (1971).